Calibration Free Upper Limb Joint Motion Estimation Algorithm with Wearable Sensors

Max van Lith*†, Justin Fong*, Vincent Crocher*, Ying Tan*, Iven Mareels* and Denny Oetomo*
*Melbourne School of Engineering, The University of Melbourne, Parkville VIC 3010, Australia
Email: {justinf, vcrocher,yingt,i.mareels, doetomo}@unimelb.edu.au
†Eindhoven University of Technology, Department of Mechanical Engineering, Eindhoven, The Netherlands
Email: m.m.g.v.lith@student.tue.nl

***Abstract*—This paper aims to establish a post processing algorithm to estimate the upper limb motion, given a set of measurements from wearable sensors representing the orientation of the shoulder, upper arm and lower arm. The motivation of the development is the measurement of the upper limb motion for subjects with motor impairments, such as post-stroke patients preventing the use of specific motions for calibration purposes and allowing the sensors to be relatively insensitive to their mounting positions. The type of sensors has been left general, with the experimental validation in this paper carried out using inertial sensors and magnetic trackers. The method is validated both numerically and experimentally, and shows improvements compared to the common inverse kinematics approach, especially in the practical conditions where sensor mounting alignment is suboptimal.**

I. Introduction

In the measurement of human body motion, a motion capture system typically records the spatial positions of a set of markers attached to a body part or segment acquire data representing individual body features (e.g. in the case of RGBD camera based systems). A kinematic model of the articulation of the human body is then generally constructed. The joint motion estimation is therefore the process of obtaining the values of the joint displacements of the kinematic model from the marker or feature displacements obtained by the motion capture system. This can be achieved by performing Inverse Kinematics (IK) analyses on the obtained motion capture data. Motion capture and motion estimation have several relevant applications in modern society. One example is the field of motor function rehabilitation [2], [3], where joint motion tracking can help physicians and researchers gain insight into the mechanisms of body movements or the quantification of the interaction results with relevant technologies, such as rehabilitation robotics [4], [5]. The work in this paper was initially motivated by clinical needs to assist in the quantification of patients movements.

Since the 1980s, much research has been conducted on obtaining and analysing the motion capture data [7], [8], [9], [10]. The data capture process has been performed using different modalities of measurements: inertial measurement units (IMUs) [11], magnetic trackers [5] or optical systems [10]. Each mode of measurement has its strengths and challenges to suit particular applications. IMUs allow the flexibility of being completely mobile while suffering from relatively high level of measurement noise and drift. Magnetic trackers are bound in terms of their workspace but provide high accuracy measurements without drift. Markerless optical systems — e.g. RGBD cameras — do not require any calibration posture or movement when coupled with appropriate algorithms but demonstrate relatively lower reliability and accuracy [12]. Their marker based counterpart, while capable of high accuracy, suffers from longer setup and data post-processing time. All optical systems are also confined to a specific space instrumented with the cameras and prone to occlusions.

This paper seeks to address the technical challenges arising from a specific application: namely the assessment of the motor functionality of subjects suffering from upper limb motor impairment, such as those caused by stroke. The condition of the subjects involved in the measurement and the practicality of the motion capture exercise dictate the unique requirements from which the joint motion estimation is constructed. The primary challenge is the difficulty in the subject performing both voluntary and involuntary movements which prevents the use of any specific calibration posture. Furthermore, the process is required to be relatively insensitive to the sensing units location since subjects may be required to place the sensors themselves. Joint motion tracking strategies today generally still rely on calibration processes [11], [13] or require specific locations for the sensing unit or markers [14], thus reducing their effectiveness as a practical day to day tool.

The development of accurate, cost-efficient and easy-to-use joint motion tracking methods is important in the area of motor rehabilitation [6] where kinematic measurements of patients are today limited to the clinical context or even to laboratory settings due to their complexity. Collection of accurate kinematic data over long periods of time, for example during a patient's hospital stay or after their discharge to their home environment, could provide important information to researchers and clinical practitioners [2]. This can lead to a direct benefit in the design of more targeted treatments and for recovery evaluation.

The method proposed in this paper computes the joint angular displacement of the kinematic model representing the upper limb of a subject given a set of motion capture data. The method can be applied to any modality of motion capture which provides the sensors orientation at the points of measurement (e.g. portable IMUs, magnetic trackers). As

TABLE I: Classical Denavit-Hartenberg parameters for the kinematic model of the upper limb.

i	a_i	α_i	d_i	θ_i	Description	Joint limits
1	0	$\pi/2$	0	q_1	Plane of elevation	$[-\pi, \pi]$
2	0	$-\pi/2$	0	q_2	Elevation	$[-\pi, 0]$
3	0	$\pi/2$	l_{ua}	q_3	Axial rotation upper arm	$[-\pi, \pi]$
4	0	$\pi/2$	0	q_4	Elbow	$[\ 0, \pi]$
5	0	0	l_{la}	q_5	Forearm	$[-\pi, \pi]$

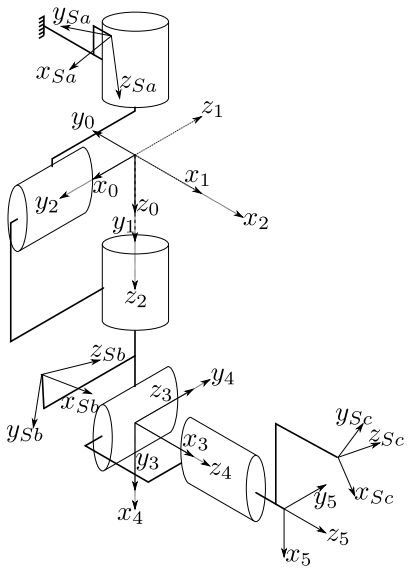

Fig. 1: Kinematic model of the upper limb, for $\mathbf{q} = \begin{pmatrix} -\frac{\pi}{2} & 0 & 0 & \frac{\pi}{2} & 0 \end{pmatrix}^T$, with sensor Sa attached to the shoulder, sensor Sb attached to the upper arm and sensor Sc attached to the forearm.

such, the outcomes of this paper have the direct potential of providing joint estimation information to help resolve the needs identified above.

The rest of this paper is structured as follows. The problem formulation and limitations of the Inverse Kinematic (IK) solutions are introduced in Section II. Section III describes the proposed solution. Results of numerical simulations and of two practical experiments are presented in Section IV. Finally, discussions and conclusions are presented in Section V.

II. Problem Definition

In this study, the kinematic model of the subjects upper limb is considered as a 5 dof serial kinematic chain, articulated by revolute joints. The generalized coordinates of the joints are denoted by $\mathbf{q} \in \mathbb{R}^{5\times 1}$. Table I provides the Denavit-Hartenberg parameters [15] of the kinematic model and the associated clinical terminologies of the joints [16] and their limits. Fig. 1 provides a schematic of the kinematic model.

The first three joints correspond to the spherical joint of the idealised *gleno-humeral* (shoulder) joint. The fourth and fifth joints represent the elbow flexion/extension and pronation/supination, respectively. The model is only derived up to the forearm — wrist and finger motions are not considered.

In this study, the problem of joint motion estimation is defined as: given the upper limb Forward Kinematics (FK) and its parameters $\mathbf{p}_c$ (constant for a given subject), obtain the set of N joint configurations $\mathbf{q}_n = \begin{pmatrix} q_{1,n} & \dots & q_{5,n} \end{pmatrix}^T, 1 \leq n \leq N$ which minimize the error between the FK of this set of $\mathbf{q}_n$ and the orientations of the sensors for these N measurements.

As stated in Section I, the application of joint motion tracking to subjects with upper limb motor impairment imposes certain requirements to the design of a solution. The main design requirements therefore are that the resulting technique

- requires no calibration posture to be performed by the wearer
- is insensitive to where the sensor is placed on the shoulder and along the upper arm and forearm
- demonstrates as much as possible robustness to the misalignment of the sensors.

Moreover it is assumed that the motion capture is performed using three sensor units: Sensor Sa placed on the shoulder, sensor Sb attached to the upper arm anywhere above the elbow and sensor Sc attached to the forearm — as close as possible to the wrist. Therefore, Sa, Sb and Sc are modelled to be rigidly attached to links $i = 0, 3$ and 5 respectively (see Fig. 1). All sensors provide data with respect to the global frame B.

As the primary objective is to obtain the motion of the upper limb with respect to the body, the motion of the body trunk, represented by Frame 0 is not considered in this paper.

The origin of sensor Sa is described with respect to Frame 0 at the shoulder with translational displacements x_{Sa}, y_{Sa}, z_{Sa} and angular displacements in the form of roll, pitch, and yaw angles $\phi_{Sa}, \psi_{Sa}, \theta_{Sa}$. The displacements would be constant throughout if the shoulder joint was an ideal spherical joint, which is not the case in practice. Sensor Sb is rigidly attached to Link 3, corresponding to the upper arm. The offsets are given by x_{Sb}, y_{Sb}, z_{Sb} describing translation and roll, pitch, and yaw angles $\phi_{Sb}, \psi_{Sb}, \theta_{Sb}$ describing rotation w.r.t. Frame 3. For sensor Sc, the offsets are described with x_{Sc}, y_{Sc}, z_{Sc} (translation) and roll, pitch, and yaw angles $\phi_{Sc}, \psi_{Sc}, \theta_{Sc}$ (rotation), w.r.t. Frame 5. Sensor Sc is rigidly attached to Link 5, which corresponds to the forearm.

The short notation $s_\beta = \sin(\beta)$ and $c_\beta = \cos(\beta)$ is used throughout this paper. For the transformation between two consecutive links of the kinematic model, the homogeneous transformation matrix describing the rotation and position of Frame i w.r.t. Frame $i-1$ is denoted by $\mathbf{T}_i^{i-1}$, as defined in [15]. Translational offsets are denoted x, y, z and the rotational offsets are expressed as roll, pitch, and yaw angles and denoted ϕ, ψ, θ. Arm lengths and offsets of base and sensors, are constant for a given dataset. These constant parameters are referred to as $\mathbf{p}_c$.

The forward kinematics (FK) of the three sensor frames w.r.t. the base frame B can be modelled as:

$$FK(\mathbf{p}_c, \mathbf{q}) = \begin{cases} \mathbf{T}_{Sa}^B = \mathbf{T}_0^B \mathbf{T}_{Sa}^0 \\ \mathbf{T}_{Sb}^B = \mathbf{T}_0^B \mathbf{T}_1^0 \mathbf{T}_2^1 \mathbf{T}_3^2 \mathbf{T}_{Sb}^3 \\ \mathbf{T}_{Sc}^B = \mathbf{T}_0^B \mathbf{T}_1^0 \mathbf{T}_2^1 \mathbf{T}_3^2 \mathbf{T}_4^3 \mathbf{T}_5^4 \mathbf{T}_{Sc}^5 \end{cases} \quad (1)$$

Let $\mathbf{R}_y^x$ be the rotational part of a homogeneous transformation matrix $\mathbf{T}_y^x$, which are the first three rows and columns, and ${}_{ij}R_y^x$ be the element of $\mathbf{R}_y^x$ on the i'th row and the j'th column. Let $X = c_\beta, Y = s_\beta$, then $\text{atan2}(X, Y) = \beta$.

The conventional IK are based on the assumption that the sensor frames are aligned with the link frames to which they are rigidly attached (i.e., $\mathbf{R}_{Sa}^0 = \mathbf{R}_{Sb}^3 = \mathbf{R}_{Sc}^5 = \mathbf{I}$). In this study, the IK are calculated using rotation matrices $\mathbf{R}_{Sb}^{Sa}$ and $\mathbf{R}_{Sc}^{Sb}$. The rotation matrix of sensor Sb w.r.t. Sa is given by:

$$\mathbf{R}_{Sb}^{Sa} = \left(\mathbf{R}_{Sa}^{B}\right)^{-1}\mathbf{R}_{Sb}^{B} = \begin{pmatrix} c_{q_1}c_{q_2}c_{q_3} - s_{q_1}s_{q_3} & -c_{q_1}s_{q_2} & c_{q_3}s_{q_1} + c_{q_1}c_{q_2}s_{q_3} \\ c_{q_1}s_{q_3} + c_{q_2}c_{q_3}s_{q_1} & -s_{q_1}s_{q_2} & c_{q_2}s_{q_1}s_{q_3} - c_{q_1}c_{q_3} \\ c_{q_3}s_{q_2} & c_{q_2} & s_{q_2}s_{q_3} \end{pmatrix} \quad (2)$$

From (2), the plane of elevation can be estimated with:

$$\bar{q}_1 = \text{atan2}(-{}_{12}R_{Sb}^{Sa}, -{}_{22}R_{Sb}^{Sa}) = \text{atan2}(c_{q_1}s_{q_2}, s_{q_1}s_{q_2}) \quad (3)$$

Now, using $\bar{q}_1$ and (2), the elevation can be obtained with:

$$\bar{q}_2 = \text{atan2}\left({}_{32}R_{Sb}^{Sa}, \frac{-{}_{12}R_{Sb}^{Sa}}{c_{\bar{q}_1}}\right) = \text{atan2}(c_{q_2}, s_{q_2}) \quad (4)$$

From (2), the axial rotation of the upper arm can be found with:

$$\bar{q}_3 = \text{atan2}({}_{31}R_{Sb}^{Sa}, {}_{33}R_{Sb}^{Sa}) = \text{atan2}(c_{q_3}s_{q_2}, s_{q_2}s_{q_3}) \quad (5)$$

Because of the order of revolute joints in the kinematic model, there are two solutions for $\bar{q}_1, \bar{q}_2, \bar{q}_3$. This redundancy is resolved by ensuring that the joint angles comply with the assumed joint limits of Table I.

The elbow angle is computed using the vector pointing along the upper arm ($\mathbf{y}_{Sb}$) and the vector pointing along the forearm ($\mathbf{z}_{Sc}$):

$$\bar{q}_4 = \text{atan2}\left(\mathbf{y}_{Sb} \cdot \mathbf{z}_{Sc}, |\mathbf{y}_{Sb} \times \mathbf{z}_{Sc}|_2\right) = \text{atan2}(c_{q_4}, s_{q4}) \quad (6)$$

For the forearm joint, the following rotation matrix is used:

$$\mathbf{R}_{Sc}^{Sb} = \left(\mathbf{R}_{Sb}^{B}\right)^{-1}\mathbf{R}_{Sc}^{B} = \begin{pmatrix} c_{q_4}c_{q_5} & -c_{q_4}s_{q_5} & s_{q_4} \\ c_{q_5}s_{q_4} & -s_{q_4}s_{q_5} & -c_{q_4} \\ s_{q_5} & c_{q_5} & 0 \end{pmatrix} \quad (7)$$

Using (7), the forearm angle is calculated with:

$$\bar{q}_5 = \text{atan2}\left({}_{32}R_{Sb}^{Sb}, {}_{31}R_{Sc}^{Sb}\right) = \text{atan2}(c_{q_5}, s_{q_5}) \quad (8)$$

Note that there is a singularity for $s_{q_2} = 0$ and that numerical issues may arise when $s_{q_2} \approx 0$ or $c_{\bar{q}_1} \approx 0$. The output of the IK is denoted with $\bar{\mathbf{q}} = \begin{pmatrix}\bar{q}_1 & \bar{q}_2 & \bar{q}_3 & \bar{q}_4 & \bar{q}_5\end{pmatrix}^T$.

As mentioned before, the presented IK solution is based on the assumption that the sensors are aligned with the links of the kinematic model — or that the misalignment offsets are known. Due to modelling errors, the shape of human limbs and the elasticity of the human muscles and skin, the misalignment is impractical to quantify. To illustrate the effect of applying the IK with sensor Sa misaligned, numerical simulations were performed. For every trial, random joint configurations $\mathbf{q}^*$ were sampled from a uniform distribution, conforming to the joint limits. Singular positions were discarded with $\left|c_{q_1^*}\right| > 10^{-4}$ and $s_{q_2^*} < -10^{-4}$. The constant rotational offset of sensor S_a was sampled from a uniform distribution with four different bounds: $b = \{1°, 5°, 10°, 20°\}$ and such that for every sample $\left|\begin{pmatrix}\phi_{Sa}^* & \psi_{Sa}^* & \theta_{Sa}^*\end{pmatrix}\right|_2 = b$. The true constant parameters are denoted $\mathbf{p}_c^*$. Using $\mathbf{q}^*$ and $\mathbf{p}_c^*$, the FK was calculated with (1). Subsequently, $\bar{\mathbf{q}}$ was obtained with (3), (4), (5), (6) and (8). This was repeated for 10^5 trials for every offset. Subsequently, histograms of the error $\mathbf{q}^* - \bar{\mathbf{q}}$ were obtained. The results for the plane of elevation are presented in Fig. 2a, for the elevation in Fig. 2b, for the axial rotation of the upper arm in Fig. 2c.

TABLE II: Percentage of joint estimation errors within the bounds of sensor offset angles, using the conventional IK solution.

	$b = 1°$	$b = 5°$	$b = 10°$	$b = 20°$
q_1	77.76%	67.99%	66.12%	65.25%
q_2	100%	100%	100%	100%
q_3	77.87%	68.32%	66.35%	65.41%

It can be concluded from Fig. 2 that the accuracy of the estimation of shoulder joint displacements suffers from the offset and misalignment in sensor Sa when the conventional IK method is applied, where a small misalignment may cause large estimation errors. This is particularly true for q_1 and q_3, for which a significant portion of the resulting trial errors was observed to be larger than the sensor offset itself. The percentages of joint estimation errors that are smaller than or equal to the bound b of sensor offsets are given in Table II.

III. Proposed method

The previously described conventional IK method calculates $\bar{\mathbf{q}}_n$ using only measurement n. This study proposes subsequently using N measurements and N calculated $\bar{\mathbf{q}}_n$ to identify the orientation $\hat{\mathbf{R}}_{Sa}^0$ of sensor Sa relative to Frame 0 —through the roll, pitch, yaw equivalents $\hat{\phi}_{Sa}, \hat{\psi}_{Sa}, \hat{\theta}_{Sa}$. The data of sensor Sa can now be transformed to $\hat{\mathbf{R}}_0^B = \mathbf{R}_{Sa}^B\left(\hat{\mathbf{R}}_{Sa}^0\right)^{-1}$. Calculating the IK again using $\hat{\mathbf{R}}_0^B, \mathbf{R}_{Sb}^B, \mathbf{R}_{Sc}^B$ results in N values for $\hat{\mathbf{q}}_n$. Recall that the IK are based on the assumption that the sensor frames are aligned with the link frames to which these sensors are attached — or that the misalignment offsets are known. Fig. 2 implies that the resulting joint motion estimation $\hat{\mathbf{q}}_n$ is more accurate than $\bar{\mathbf{q}}_n$ if $\hat{\mathbf{R}}_0^B$ better approximates $\mathbf{R}_0^B$, compared to $\mathbf{R}_{Sa}^B$. The conventional IK solution and the proposed method are depicted schematically in Fig. 3.

The identification of $\hat{\phi}_{Sa}, \hat{\psi}_{Sa}, \hat{\theta}_{Sa}$ is achieved by implementing the geometric identification method as described in [17]. It is given in **Algorithm 1**. Note that subscript n is added to matrices to refer to sample n, and subscript k to indicate iteration k.

In **Algorithm 1**, the orientation of sensor Sa is referred to with $\mathbf{p}_k = \begin{pmatrix}\phi_{Sa,k} & \psi_{Sa,k} & \theta_{Sa,k}\end{pmatrix}^T$. The angular displacement errors $\mathbf{\Omega}$ are obtained with $f(\mathbf{E})$, where $f()$ converts a rotation matrix to roll, pitch and yaw angles. The estimation error at iteration k is referred to with $\Delta\mathbf{X}_k$. Furthermore, let $\mathbf{J}_k$

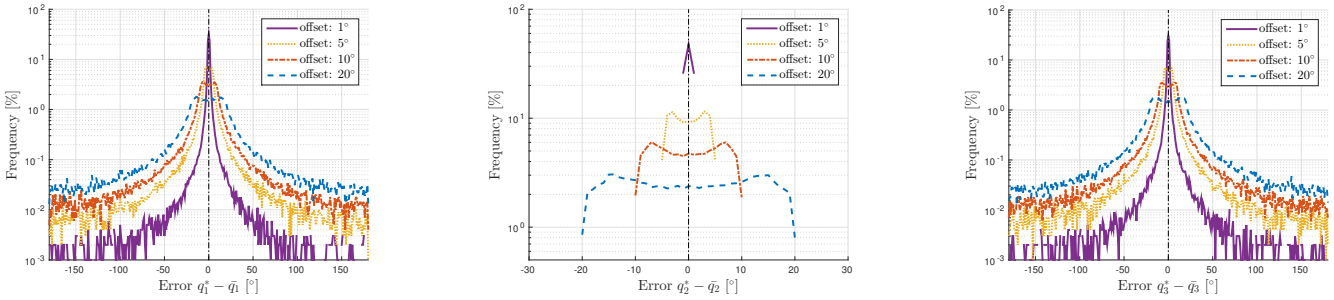

(a) Plane of elevation ($q_1^* - \bar{q}_1$). (b) Elevation ($q_2^* - \bar{q}_2$). (c) Axial rotation ($q_3^* - \bar{q}_3$).

Fig. 2: Distribution of error in the conventional IK solution

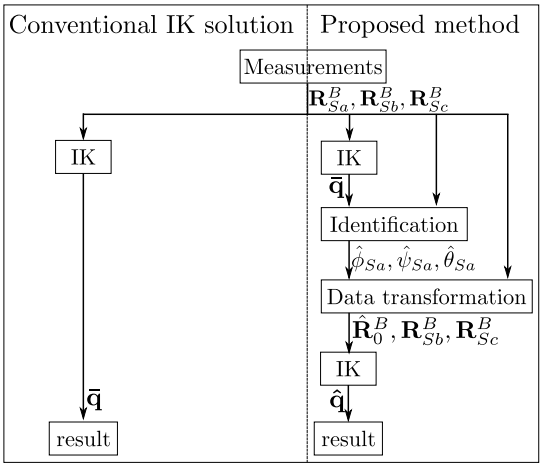

Fig. 3: Schematic representation of the joint tracking solutions, summarising both the conventional IK solution and the proposed method.

be the Jacobian at the kth iteration such that $\Delta\mathbf{X}_k = \mathbf{J}_k \Delta\mathbf{p}_k$ relates a small change in the estimated parameters $\mathbf{p}_k$ to the corresponding change in $\mathbf{X}_k$.

IV. Validation

For all validations performed, **Algorithm 1** was applied with the following criteria. The while-loop breaks for $\left|\Delta\mathbf{X}_{\hat{k}}\right|_\infty < 3°$ and $k_{max} = 10$. Update $\hat{k}$ if $rms(\Delta\mathbf{X}_k) < rms(\Delta\mathbf{X}_{\hat{k}})$, and $\delta k = 3$. Step size α_k was chosen s.t. $|\alpha_k \delta\mathbf{p}_k|_2 \leq 1$.

Algorithm 1 Identification of $\hat{\phi}_{Sa}, \hat{\psi}_{Sa}, \hat{\theta}_{Sa}$

$k = 0$
$\hat{k} = 0$
$\mathbf{p}_0 = \begin{pmatrix} 0 & 0 & 0 \end{pmatrix}^T$
while $\Delta\mathbf{X}_{\hat{k}} \geq$ tolerance **and** $k < k_{max}$ **do**
  for $n = 1$ **to** N **do**
    $(\mathbf{T}_{Sa,n,k}^B, \mathbf{T}_{Sb,n,k}^B, \mathbf{T}_{Sc,n,k}^B) = FK(\mathbf{p}_{c,k}, \bar{\mathbf{q}})$ using (1)

$$\begin{pmatrix} \mathbf{E}_{n,k}^{Sa} \\ \mathbf{E}_{n,k}^{Sb} \\ \mathbf{E}_{n,k}^{Sc} \end{pmatrix} = \begin{pmatrix} \mathbf{R}_{Sa,n}^B \left(\mathbf{R}_{Sa,n,k}^B\right)^{-1} \\ \mathbf{R}_{Sb,n}^B \left(\mathbf{R}_{Sb,n,k}^B\right)^{-1} \\ \mathbf{R}_{Sb,n}^B \left(\mathbf{R}_{Sb,n,k}^B\right)^{-1} \end{pmatrix}$$

$$\Delta\mathbf{X}_{n,k} = \begin{pmatrix} \mathbf{\Omega}_{n,k}^{Sa} \\ \mathbf{\Omega}_{n,k}^{Sb} \\ \mathbf{\Omega}_{n,k}^{Sc} \end{pmatrix} = \begin{pmatrix} f(\mathbf{E}_{n,k}^{Sa}) \\ f(\mathbf{E}_{n,k}^{Sb}) \\ f(\mathbf{E}_{n,k}^{Sc}) \end{pmatrix}$$

  end for
  if $\Delta\mathbf{X}_k < \Delta\mathbf{X}_{\hat{k}}$ **then**
    $\hat{k} = k$
    if $\hat{k} = k_{max}$ **then**
      $k_{max} = k_{max} + \delta k$
    end if
  end if
  Calculate $\mathbf{J}_k$
  $\delta\mathbf{p}_k = (\mathbf{J}_k^T \mathbf{J}_k)^{-1} \mathbf{J}_k^T \Delta\mathbf{X}_k$
  choose step size α_k
  $\mathbf{p}_{k+1} = \mathbf{p}_k + \alpha_k \delta\mathbf{p}_k$
  $k = k + 1$
end while
return $\mathbf{p}_{k=\hat{k}}$

A. Computational set-up

The proposed method was evaluated by numerical simulation in the following way. Joint angles $\mathbf{q}^*$ were sampled from a uniform distribution within the previously defined joint limits. Sensor Sa offset was sampled from a uniform distribution such that $\left|\begin{pmatrix} \phi_{Sa}^* & \psi_{Sa}^* & \theta_{Sa}^* \end{pmatrix}\right|_2 = 25°$. The sensors simulated measurements were calculated with (1). To simulate the measurement noise, this was subsequently multiplied with the rotational matrix produced with ϕ, ψ, θ sampled from a uniform distribution within $\pm 5°$. This was repeated 50 times to obtain a set of simulated motion capture data. The initial guess, $\bar{\mathbf{q}}_n$, was defined using the IK with $\mathbf{p_c} = \mathbf{0_3}$. The proposed method was then applied to obtain the offset parameters $\mathbf{p}_{\hat{k}}$ and the joint angles $\hat{\mathbf{q}}_n$ for all measurements. The error in identification was defined as $\mathbf{p}_c^* - \mathbf{p}_{\hat{k}}$. The error in joint angles for one sample was defined as $\hat{\mathbf{e}}_n = \mathbf{q}_n^* - \hat{\mathbf{q}}_n$ and $\bar{\mathbf{e}}_n = \mathbf{q}_n^* - \bar{\mathbf{q}}_n$. This was repeated for 10^5 different trials.

B. Computational results

In Fig. 4, the boxplots of the errors in the identification process are given. After identification, the absolute errors of

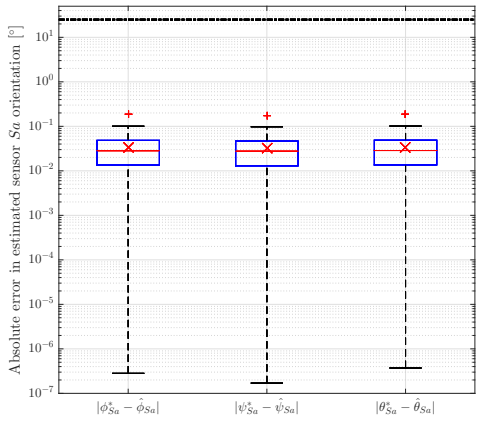

Fig. 4: Absolute error of Sa rotational offsets: $|\mathbf{p}_c^* - \mathbf{p}_{\hat{k}}|$. Dash-dotted line indicates initial sensor offsets (25°), red line indicates median, $\times$ indicates mean, $+$ indicates maximum.

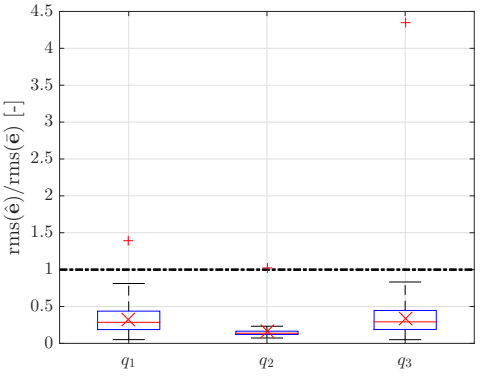

Fig. 5: Ratio of joint angle errors *rms*: $rms(\hat{\mathbf{e}})/rms(\bar{\mathbf{e}})$. Values below 1 indicate an improvement in the joint motion tracking. Red line indicates median, $\times$ indicates mean, $+$ indicates maximum.

sensor Sa orientation, roll, pitch and yaw, were observed to be below $0.2°$, with mean and median errors below $0.05°$.

Recall that for one trial the joint angle errors are $\hat{\mathbf{e}} = \mathbf{q}^* - \hat{\mathbf{q}}$ and $\bar{\mathbf{e}} = \mathbf{q}^* - \bar{\mathbf{q}}$. The ratio of $rms(\hat{\mathbf{e}})$ and $rms(\bar{\mathbf{e}})$ provides insights into the difference between the conventional method and the proposed method: a ratio smaller than 1 indicates an improvement in accuracy. The ratios are given in Fig. 5 for the three shoulder angles. Note that the distributions of the presented ratios have a long tail. At the 99th percentile, these ratios were $0.81, 0.52$ and 0.94 for q_1, q_2 and q_3 respectively.

C. Experimental set-up

The proposed method was applied to two different sets of data. In the first set, a subject was instructed to perform reaching actions while wearing three magnetic trackers (3D Guidance trakSTAR system, Ascension Technology Corporation, USA). In the second dataset, the subject was eating, using

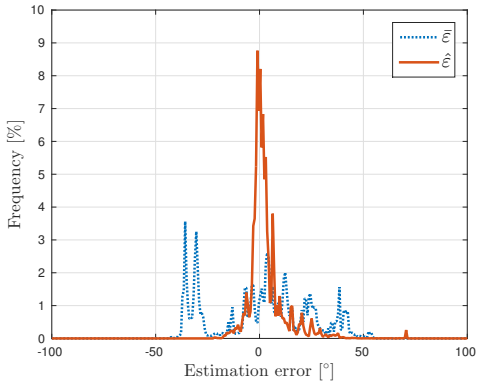

(a) First dataset, using magnetic trackers.

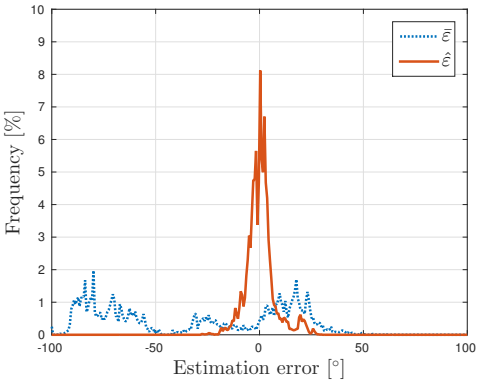

(b) Second dataset, using IMUs.

Fig. 6: Distribution of the estimation errors $\bar{\varepsilon}$ and $\hat{\varepsilon}$

knife and fork, while wearing three IMU based sensors (Opal sensors, APDM Incorporation, USA). For both datasets, the IK solutions $\bar{\mathbf{q}}$ were obtained for every sample. All sensor offsets were initialised to be zero degrees. The proposed method was used to calculate sensor Sa orientation offsets and then the joint angles $\hat{\mathbf{q}}$.

For both experiments the estimation errors $\bar{\varepsilon}$ and $\hat{\varepsilon}$ are defined as the set of the $9 \times N$ angular errors — yaw, pitch, roll for each sensor Sa, Sb, Sc, each sample n — respectively for the classic IK method and the proposed method.

D. Experimental results

For the first dataset the identification provides the following offsets: $\hat{\phi}_{Sa} = -5.1°, \hat{\psi}_{Sa} = -30.0°, \hat{\theta}_{Sa} = 24.2°$. For the second dataset, the offsets were $\hat{\phi}_{Sa} = 14.4°, \hat{\psi}_{Sa} = -68.2°, \hat{\theta}_{Sa} = -67.1°$. The distributions of $\bar{\varepsilon}$ and $\hat{\varepsilon}$ are depicted on Fig. 6. It can be observed that, for both datasets the distribution of $\hat{\varepsilon}$ is narrower than the distribution of $\bar{\varepsilon}$, indicating an improved accuracy of the joint motion tracking. Moreover, it can be observed that for the second experiment the conventional IK method produces a distribution with two peaks, around $-80°$ and $20°$ whereas the proposed method produces a zero-centred distribution.

The difference between the two methods $\mathbf{d} = \bar{\mathbf{q}} - \hat{\mathbf{q}}$ is shown in Fig. 7 as a function of time. For the first experiment, the

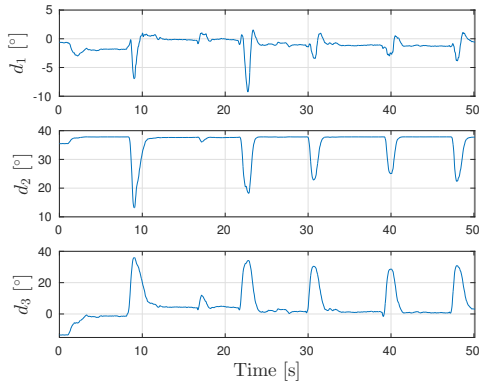

(a) First dataset, using magnetic trackers.

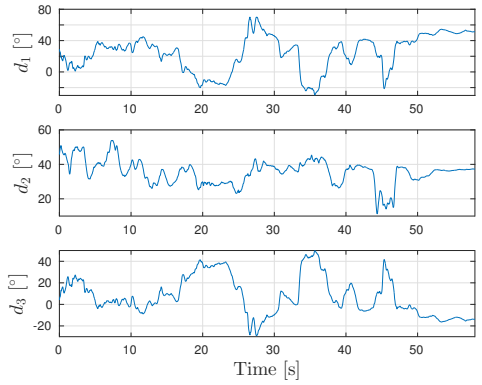

(b) Second dataset, using IMUs.

Fig. 7: Difference $\mathbf{d} = \bar{\mathbf{q}} - \hat{\mathbf{q}}$ between the common IK solutions and proposed method as a function of time for the plane of elevation (d_1), elevation (d_2) and axial rotation (d_3).

five reaching movements of the subject can be recognised by the spikes at $t = 9$, 23, 32, 40 and 47 seconds (Fig. 7a). It is also to note that differences of up to 70° can be observed for the second experiment (Fig. 7b).

V. Conclusion

A method combining the conventional IK procedure and offset identification was proposed to improve accuracy of upper limb joint motion tracking when calibration postures cannot be used. The method estimates the orientation offsets of the shoulder sensor — due to positioning misalignment — providing a more robust motion estimation method. The method also does not require any translational displacement information from the sensor units, relying solely on the orientation measurement. This allows the sensor units to be placed anywhere along the upper arm and forearm, as well as the shoulder, where the orientation on the shoulder is identified automatically as part of the proposed method.

The proposed solution was applied to both simulated and measured motion capture data to evaluate its performance. In over 99% of the simulated cases an improvement in joint motion tracking accuracy was observed. Experiments, performed with two different types of sensors, validated the practical usability and efficiency of the proposed method with notable improvements in accuracy of joint motion tracking.

The proposed method can be further generalised to identify orientation offsets of the upper arm and forearm sensors in order to further increase the accuracy of the motion tracking.

Acknowledgment

This work was supported by the Australian Research Council Discovery Project DP130100849 and DP160104018.

References

[1] D.M. Gavrila, "The visual analysis of human movement: A survey," Computer Vision and Image Understanding, vol. 73, pp. 82-98, January 1999.

[2] B. Ploderer, J. Fong, A. Withana, M. Klaic, S. Nair, V. Crocher, F. Vetere, and S. Nanayakkara, (in press). "ArmSleeve: a patient monitoring system to support occupational therapists in stroke rehabilitation". In Proc. of the Conf. on Designing Interactive Systems (DIS 2016). New York: ACM Press.

[3] A. de los Reyes-Guzman, I. Dimbwadyo-Terrer, F. Trincado-Alonso, F. Monasterio-Huelin, D. Torricelli, and A. Gil-Agudo, "Quantitative assessment based on kinematic measures of functional impairments during upper extremity movements: A review," Clinical Biomechanics, vol. 29, no. 7, pp. 719-727, August 2014.

[4] J. Fong, V. Crocher, D. Oetomo, Y. Tan and I. Mareels, "Effects of Robotic Exoskeleton Dynamics on Joint Recruitment in a Neurorehabilitation Context," in Procs. 14th IEEE/RAS-EMBS Int. Conf. on Rehabilitation Robotics, 11 - 14 August 2015, Singapore, pp. 834-839.

[5] J. Fong, V. Crocher, D. Oetomo and Y .Tan, "An Investigation into the Reliability of Upper-limb Robotic Exoskeleton Measurements for Clinical Evaluation in Neurorehabilitation," in Proc. the 7th Int. IEEE EMBS Conf. on Neural Engineering, Montpellier, 22-24 April 2015, pp. 795-798.

[6] S-H. Zhou, J. Fong, V. Crocher, Y. Tan, D. Oetomo and I. Mareels, "Learning Control in Robot-assisted Rehabilitation of Motor Skills," Journal of Control and Decision, vol. 3 issue 1, pp. 19-43, 2016.

[7] L. Wang, W. Hu and T. Tan, "Recent developments in human motion analysis," Pattern Recognition, vol. 36, pp. 585-601, 2003.

[8] H. Zhou and H. Hu, "Human motion tracking for rehabilitation - A survey," Biomedical Signal Processing and Control, vol. 3, pp.1-18, 2008.

[9] L.F. Yeung , K.C. Cheng , C.H. Fong , W.C.C. Lee and K.Y. Tong, "Evaluation of the Microsoft Kinect as a clinical assessment tool of body sway," Gait & Posture, vol. 40, pp. 532-538, 2014.

[10] A. Scano, M. Caimmi, A. Chiavenna, M. Malosio and L. Molinari Tosatti, "Kinect One-based biomechanical assessment of upper-limb performance compared to clinical scales in post-stroke patients," 37th Annu. Int. Conf. IEEE Engineering in Medicine and Biology Society, Milan, 2015, pp. 5720-5723.

[11] A.G. Cutti, A. Giovanardi, L. Rocchi and A. Davalli, "Motion analysis of the upper-limb based on inertial sensors: Part 1 - Protocol description," Journal of Biomechanics, vol.40, pp.S250, 2007.

[12] A. Pfister, A.M. West, S. Bronner, and J. A. Noah, "Comparative Abilities of Microsoft Kinect and Vicon 3D Motion Capture for Gait Analysis, Journal of Medical Engineering & Technology 38, vol.38, no. 5, pp. 274-280, May 2014.

[13] D. Roetenberg, H. Luinge and P. Slycke, "Xsens MVN: full 6DOF human motion tracking using miniature inertial sensors," Xsens Motion Technologies BV, Technical Report, April 2013.

[14] *Vicon 512 User Manual*, Vicon Motion Systems, Tustin CA, January 1999.

[15] M.W. Spong, S. Hutchinson and M. Vidyasagar, *Robot Modeling and Control*, New York: Wiley, November 2005.

[16] G. Wu et al., "ISB recommendation of definitions of joint coordinate systems of various joints for the reporting of human joint motion - Part II: shoulder, elbow, wrist and hand," Journal of Biomechanics, vol. 38, pp. 981-992, 2005.

[17] W. Khalil, and E. Dombre, *Modeling, Identification and Control of Robots*, Oxford: Butterworth-Heinemann, 2004.